VII International Conference on Computational Methods for Coupled Problems in Science and Engineering
COUPLED PROBLEMS 2017
M. Papadrakakis, E. Oñate and B. Schrefler (Eds)

NUMERICAL SIMULATIONS OF MICRO JETS PRODUCED WITH A DOUBLE FLOW FOCUSING NOZZLE

GREGA BELŠAK[1], SAŠA BAJT[2], KENNETH R. BEYERLEIN[3] AND BOŽIDAR ŠARLER[1,4]

[1] Laboratory for Simulation of Materials and Processes
Institute of Metals and Technology
Lepi pot 11, SI-1000 Ljubljana, Slovenia
email: grega.belsak@imt.si

[2] Photon Science
Deutsches Elektronen-Synchrotron DESY
Notkestraße 85, 22607 Hamburg, Germany
email: sasa.bajt@desy.de

[3] Center for Free-Electron Laser Science
Deutsches Elektronen-Synchrotron DESY
Notkestraße 85, 22607 Hamburg, Germany
email: kenneth.beyerlein@cfel.de

[4] Laboratory for Fluid Dynamics and Thermodynamics
Faculty of Mechanical Engineering
University of Ljubljana
Aškerčeva c. 6, SI-1000 Ljubljana, Slovenia
email: bozidar.sarler@fs.uni-lj.si

Key words: Multiphase Flow, Micro Jet, Double Flow Focusing Nozzle

Abstract. Stable and reliable micro jets are important for many applications. Double flow focused micro jets are a novelty with an important advantage of significantly reduced sample consumption. Numerical simulations of double flow focused micro jets are a highly complex task. They represents a great computational challenge due to the multiphase nature of the problem, strong coupling between the gas and the two liquids and the sub-micron size cells needed. Simulations were performed with the open source computational fluid dynamics toolbox called OpenFOAM. Two multiphase solvers were used, one of which was modified in order to properly describe the interface between the focusing liquid and the gas. In this study two different incompressible physical models were considered and compared. A model with no mixing of the two fluids (multiphaseInterFoam solver) and a model where the diffusion of the two fluids is permitted (modified interMixingFoam solver). The results of simulations for the two different physical models using the same inlet parameters are presented. Additionally, a parametric analysis for the mixing case was performed to study the effects of different parameters on the jet formation. Particularly how the different diffusion values couple with the jet length, diameter and its stability. Results show a match in jet diameter and jet length for both models when the same set of parameters is used.

1 INTRODUCTION

Controlled production of liquid jets by means of a co-flowing immiscible fluid stream can have diverse technical applications. One of these applications is in the field of X-ray serial crystallography. Nozzles that create stable, long and fast jets of just a few micrometres in diameter are needed to deliver protein nanocrystals into the intense X-ray beam. X-rays scattered off these crystals create diffraction patterns that are recorded on a detector. Reconstructed diffraction images provide the atomic resolution protein structure. The main bottleneck in the protein structure determination is the sample preparation, especially for the membrane proteins which do not like to form larger crystals. Serial femtosecond crystallography with x-ray free electron lasers (FEL) opened up the possibly to obtain protein structures also from nanocrystals, which were previously too small for standard X-ray crystallography. Nevertheless, samples are hard to prepare and the amount of the material is very limited. It is critical to develop ways of using the minimum amount of sample material. Delivering such nanocrystals to the X-ray beam in a form of a micro jet proved to have several advantages [1]. Here, we are particularly interested in understanding the nozzle geometry that creates these micro jets. In the past such nozzles were prepared manually, which was time consuming, non-reproducible and limited to simple designs. Ceramic micro-injection moulded nozzles were a step forward ensuring reproducibility and faster assembly [2]. However, because of the high cost of the moulding tools it is desirable to test new designs before investing in a new moulding tool. Recently, a 3D printing technology enabled printing of macroscopic nozzles with a very high precision [3]. These nozzles can be used either for testing a new design or in final application. The development of numerical models presented here, gives an insight in the fluid dynamics of such systems and should help to improve future nozzle designs.

2 DOUBLE FLOW FOCUSING NOZZLE DESIGN

Early experiments were performed using gas dynamic virtual nozzles (GDVN) [4]. This nozzle structure uses two phases to create a stable micro jet:

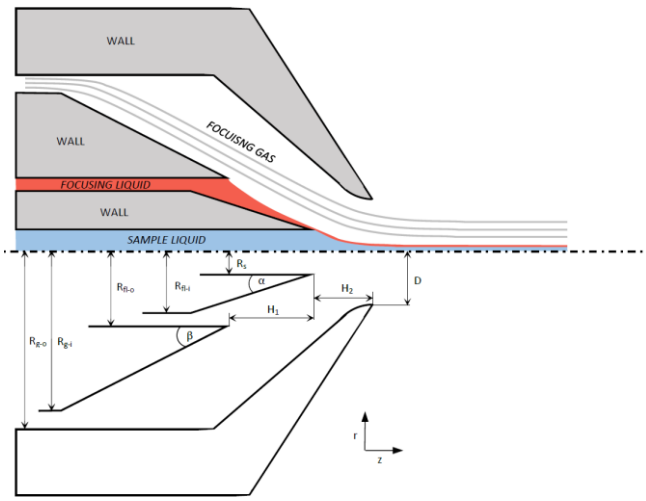

Figure 1: Graphical representation of the double flow focusing nozzle. Typical values are: R_s= 20 µm, $R_{fl\text{-}i}$= 55 µm, $R_{fl\text{-}o}$= 62 µm, $R_{g\text{-}i}$= 175 µm, $R_{g\text{-}o}$= 245 µm, α =17.5°, β= 25°, H_1= 70 µm, H_2= 85 µm, D= 35 µm.

a liquid sample fluid (nanocrystals dispersed in water) and a focusing gas (helium). In such set-up two capillaries are inserted into the nozzle. The central capillary that ends almost at the nozzle orifice is used to deliver sample liquid, while the gas is delivered through the second capillary that ends further upstream of the nozzle tip. The high pressure gas focuses the liquid into a micro jet when flowing through a small nozzle orifice. This approach typically requires sample fluid flow rates of around 20-40 µl/min.

In order to reduce the sample fluid consumption a novel double flow focusing nozzle (DFFN), depicted in figure 1, was developed [5,6]. This approach uses an additional fluid (alcohol) to further focus the sample fluid. The main advantage of using alcohol is its lower surface tension in comparison to water. It acts as a sheath liquid encapsulating the water jet, resulting in extension of the jet length by mitigating its breakup. In this way the sample fluid flow rate can be reduced to around 5 µl/min.

3 GOVERNING EQUATIONS

The multiphase model of isothermal and incompressible flow is governed by the sets of momentum and mass conservation equations for each of the phases *i*:

$$\frac{\partial(\rho_i \alpha_i \vec{u_i})}{\partial t} + \left(\rho_i \alpha_i \vec{u}_i \cdot \nabla\right)\vec{u}_i = -\alpha_i \nabla p + \nabla \cdot \left(\mu_i \alpha_i \nabla \vec{u}_i\right) + \rho_i \alpha_i \vec{g} + \vec{F}_{s,i} \tag{1}$$

$$\frac{\partial \alpha_i}{\partial t} + \vec{u_i} \cdot \nabla \alpha_i = 0 \tag{2}$$

where velocity, phase fraction, density, viscosity and surface tension force for phase *i* are given by $\vec{u}_i$, α_i, ρ_i, μ_i, $\vec{F}_i$, respectively and $\vec{g}$ is gravity. The interface compression method [7] is implemented by adding an additional compression term to the mass conservation equation in order to compress the volume fraction field and maintain a sharp interface between the phases.

$$\frac{\partial \alpha_i}{\partial t} + \vec{u_i} \cdot \nabla \alpha_i + \nabla \cdot \left(\vec{u}_c \alpha_i \left(1 - \alpha_i\right)\right) = 0 \tag{3}$$

Compression velocity $\vec{u}_c$ is applied normally to the interface.

4 NUMERICAL PROCEDURE

Numerical simulation of DFFN micro jets is a highly complex task. Multiphase nature of the problem, strong coupling between the gas and the liquids, the sub-micron size cells needed for high resolution and proper capturing of the flow all represent a great computational challenge. Because of the microscopic nature of the nozzle structure and the physical properties of the fluids used, the Reynolds number is low and therefore the flow is considered laminar. The fluids are considered to be of a Newtonian nature. The chapter is divided into three specific parts, each one describing in details the performed work.

4.1 Pre-processing

The computer model of a DFFN was prepared with FreeCAD, an open-source parametric 3D CAD modeler [8]. Non-axial symmetry of the nozzle structure (circular inner capillary inserted into square middle capillary inserted into circular outer capillary), was treated as axially symmetric (circular inner capillary inserted into circular middle capillary inserted into circular outer capillary) while keeping the cross-sectional area of the channel equal as seen in figure 2 . In this way a three dimensional problem was reduced to a two dimensional one, thus greatly reducing the calculation time and making simulations of micro jets feasible.

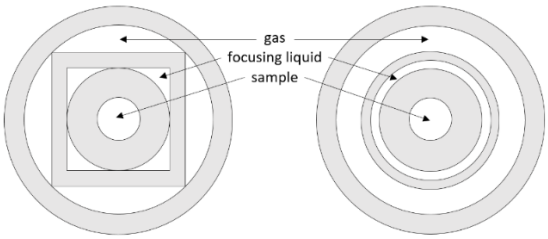

Figure 2: Transformation of the real geometry of the nozzle to axis symmetry.

For the preparation of the high quality mesh the utility called snappyHexMesh was used, which is a part of the open source computational fluid dynamics (CFD) toolbox called OpenFoam [9]. A sample mesh can be seen in figure 3. For the simulations to be run in a reasonable time (up to few days) on a modern computer with approximately 30 cores the number of cells needed to be kept as low as possible. This proved to be a difficult task for two reasons. The first reason is the desired high resolution in the jet region. Experiments show that the typical jet diameter for a DFFN is between 3 and 5 μm. At least 10 cells are needed to properly describe the fluid flow and the four interfaces between the two liquid phases. This constrains the maximal cell size to 0.5 μm. Therefore, a cell size of 0.15 μm was chosen in this study. To keep the computing time reasonable we used the finest mesh only in the area where the jet was expected to form and a coarser mesh elsewhere. The second reason is that the vacuum chamber, the area where the jet leaves the nozzle, needs to be large enough (few millimeters in length). This is because we are setting an artificial condition $(p = 0)$ on the outlet boundary of the vacuum chamber. In order to avoid the numerical errors and to prevent any interference of this artificial boundary condition on the jet formation, the size of the computational domain needs to be few millimeters. Those two constraints led to a mesh with the finest cell size of 0.15 μm with ~ 225 000 cells.

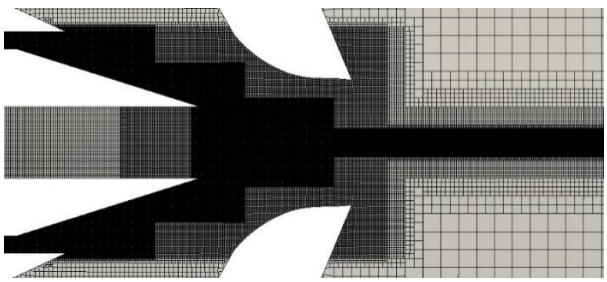

Figure 3: Representation of a mesh used in the simulations

4.2 Processing

Numerical simulations of DFFN were performed with OpenFoam (version 16.10), which has a variety of solvers available to use for many different kinds of fluid flow problems. In this study two different models were considered and hence two different solvers were used. First, a "multiphaseInterFoam" solver was used for a multiphase model where all the fluids are considered incompressible and there is no diffusion between the phases i.e. a non-mixing incompressible model. Second, a modified "InterMixingFoam" solver was used, which describes a set of three incompressible fluids two of which are miscible, i.e. a mixing incompressible model. In the later model diffusion between the sample fluid and the focusing fluid is permitted. As aforementioned the code in this solver had to be slightly modified to properly describe the interface between the focusing fluid and the gas. The inlet parameters and the physical properties of the fluids at room temperature (Table 1) were chosen to resemble the experimental values [6] and were the same in both models.

Table 1: Operating conditions and physical properties used in simulations. Values were obtained from NIST Chemistry Webbook Database

	sample liquid **WATER**	focusing liquid **ALCOHOL**	focusing gas **HELIUM**
Density [kg/m^3]	1000	789	0.33
Dynamic viscosity [kg/ms]	$1.9*10^{-5}$	$1.12*10^{-3}$	10^{-3}
Volumetric flow rate [μL/min]	5	10	/
Mass flow rate [mg/min]	/	/	21.6
Surface tension (water-gas) [N/m]		0.0728	
Surface tension (alcohol-gas) [N/m]		0.0223	
Surface tension (water-alcohol) [N/m]		0.0505	
Diffusion (water-alcohol) [N/m^2]	mixing case	10^{-9}	
	non-mixing case	0	

4.3 Post-processing

Post-processing of the simulations was performed with ParaView [10], an open source, multi-platform data analysis and visualization application. A code was written to automatically extract the jet length, diameter and concentration profile, discussed and presented in the results section. When setting up the simulation case and choosing the velocity inlet boundary conditions for the fluids a uniform axial flow (constant velocity profile) was chosen. There was a concern that this non-physical constant profile would affect the simulations. However, results demonstrated that this is not the case if the capillary is of sufficient length (above 100 μm) and the jet is monitored long enough ($t > 0.3$ ms). Under these conditions the initial constant profile changes to parabolic profile. Full development of this profile along with stabilization of the recirculation zones was used as the benchmark of a steady-state solution.

5 RESULTS

5.1 Mixing model.

The physical model, which permits the mixing between the phases, is explored here. In this three phase system the sample fluid and the focusing fluid were miscible with a diffusion constant of 10^{-9} m^2/s, which is a typical value for water-ethanol system. None of these liquids were allowed to mix with the third, gaseous phase. This model explores how diffusion affects the jet length, the diameter and the concentration profile and allows for a comparison with the experimental data [6]. In the mixing model it is challenging to distinguish between the natural (real) and the numerical (artificial) diffusion. The artificial diffusion arises from the spatial and temporal discretization of a continuous problem and therefore highly depends on the cell size and the time step. The following discretization parameters were chosen in order to keep the numerical diffusion an order of magnitude lower than the natural diffusion (10^{-10} m^2/s) and to prevent it to interfere with the results. In the region of the domain where the diffusion is present, the maximal cell size was set to 0.15 µm. The time step was controlled by setting the Courant number to the value of one, which also ensured stability of the simulation. Results are presented in figure 4.

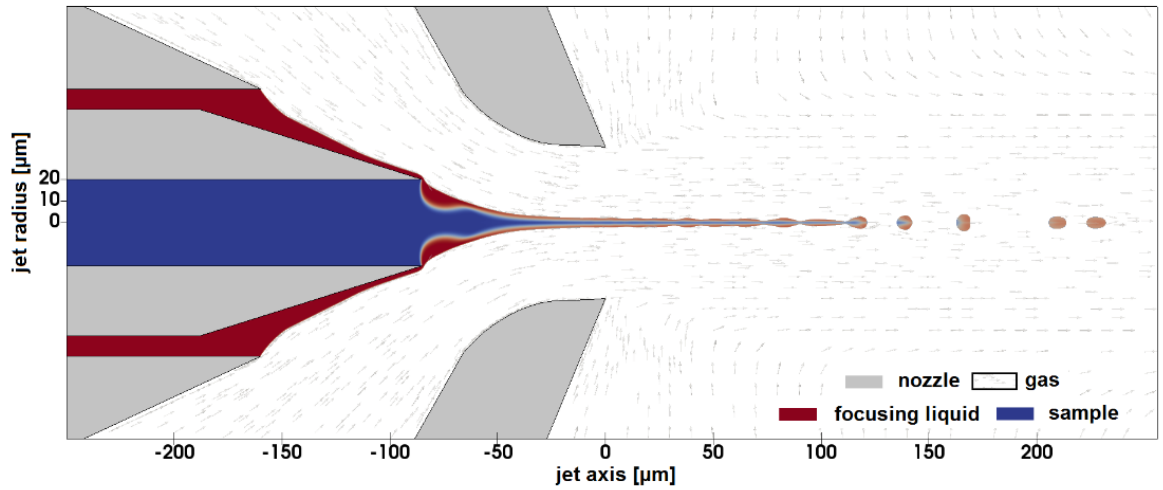

Figure 4: A snapshot of the simulation of the mixing model at time 0.4 ms. The extracted parameters are jet diameter $d_j = 4.5$ µm and average jet length $L_j = 94.2$ µm.

One of the main results of this study is the dependence of the concentration profile, which is measured at the nozzle orifice perpendicularly to the jet axis, to the varying parameters. Figure 5 shows the water concentration profile through the jet for two diffusion values. In the jet only two phases are present: water and alcohol. The total sum of both concentration phases is equal to one. It can be observed that along the jet axis (jet radius zero) the water concentration is at the highest, but still not equal to one, indicating the presence of alcohol along the jet axis. When moving towards the edges of the jet the water concentration decreases, since the alcohol concentration increases. Increasing the diffusion coefficient by an order of magnitude (green line) reduces the concentration of water around the jet axis. This is expected, since higher diffusion coefficient means more alcohol is mixed inside the water.

Results in figure 5 show a noticeable difference in the concentration profile for two diffusion values. This indicates that the observed diffused interface between the water and the alcohol is a result of natural and not numerical diffusion. It is interesting to note that changes of the diffusion coefficient do not affect the jet diameter.

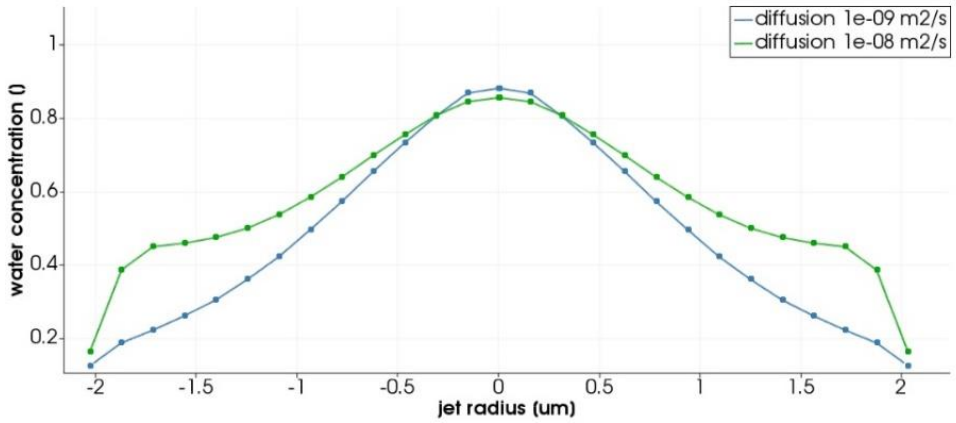

Figure 5: Water concentration profile of a jet measured at the nozzle orifice in the perpendicular direction to jet axis. Two different diffusion values are considered.

5.2 Non-mixing model.

Additionally, a multiphase model consisting of three incompressible fluids and no diffusion between the phases was explored. Results for this immiscible case are presented in figure 6.

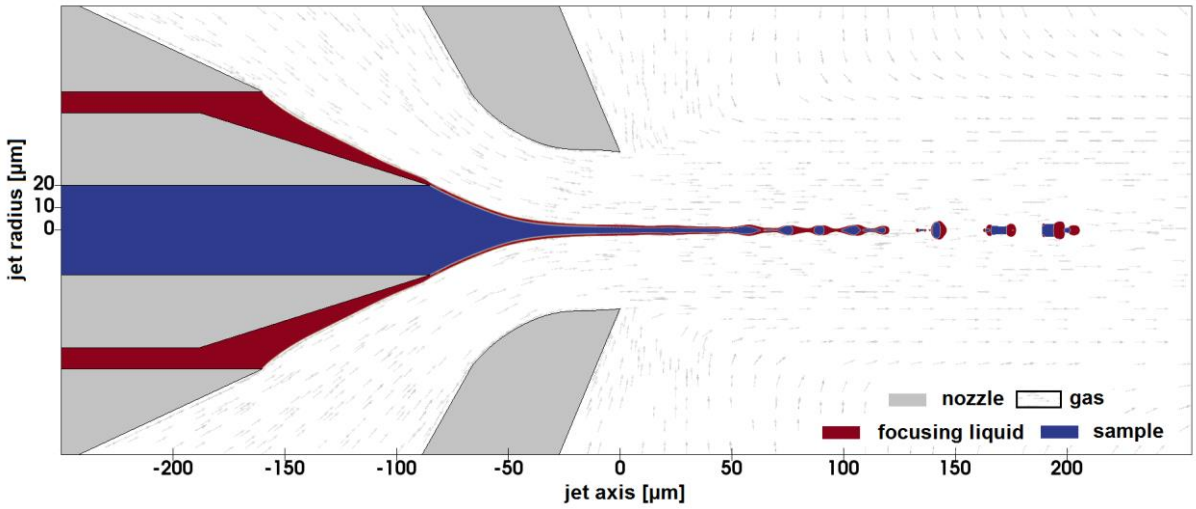

Figure 6: A snapshot of the simulation of the non-mixing model at time 0.4 ms. The extracted parameters are jet diameter $d_j = 4.8$ µm and average jet length $L_j = 97.5$ µm.

5.3 Model comparison

Results of simulations for miscible and immiscible model are presented in table 2. Calculations were performed on the same mesh under identical operating conditions and physical parameters. Findings indicate that diffusion does not affect the jet diameter and only slightly affects the jet length. Interesting thing to note is that in the non-mixing model small water droplets are forming inside the alcohol jet.

Table 2: Comparison of extracted parameters

	average jet **LENGTH** [µm]	jet **DIAMETER** [µm]
Mixing model	94.2 ± 0.3	4.5 ± 0.3
Non-mixing model	97.5 ± 0.3	4.8 ± 0.3

The surprising result is the recirculation zone in the meniscus of the jet. In an immiscible model a stable sample fluid recirculation zone is established. On the other hand in the miscible model there is no sample fluid recirculation, but only a small focusing fluid recirculation in the outermost layers of the jet as shown in figure 7.

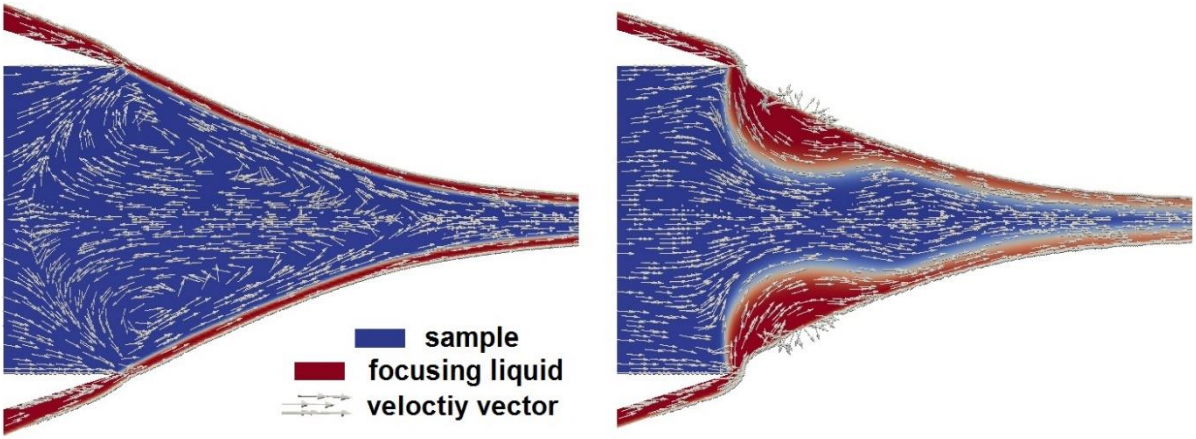

Figure 7: Comparison of recirculation zones. Left panel non-mixing model with recirculation zone. Right panel mixing model where only small recirculation occurs in the outer most layers of the focusing liquid phase.

We believe that with different operating conditions of the gas (higher gas speeds inside the nozzle) the recirculation zone would become even stronger and would also appear in the miscible case.

The numerical results published in [6] differ from the ones obtained here which we attribute to different initial conditions of the gas. In the previous work we assumed lower helium mass flow rate and inserted the gas into the nozzle under higher pressure. As a result the maximal gas velocity developed inside the nozzle orifice was around 65 m/s. Under the present operating conditions, the maximal gas velocity reaches a value of around 350 m/s, resulting in a thinner and shorter jet.

6 CONCLUSIONS

The scope of this work included numerical simulations of DFFNs. All the fluids in these simulations were considered incompressible. Experimental data [6] indicate chocked flow for the gas flowing through such DFFN into a vacuum chamber. Correct description requires a model with incompressible sample and focusing liquid, and compressible focusing gas. It is conceivable that the simulations, where the compressibility is taken into account, would result in different values of the jet diameter and length under the same initial conditions. The length of the jet is expected to change (shorten) when compressibility is added, because we would be able to describe the expansion of the high pressure gas into the low pressure vacuum chamber. This would result in higher gas velocities inside the vacuum chamber. Although not supported with full simulation, we predict that this, along with the changed gas stream shape will affect the jet length and stability. Jet diameter will also be affected by a decrease in pressure and density of gas and increased gas velocity at the nozzle orifice. Future work will include upgraded, more realistic models to address these issues.

7 ACKNOWLEDGEMENTS

We would like to thank Henry N. Chapman (CFEL, Univ. Hamburg, CUI), Dominik Oberthuer (CFEL), Juraj Knoška, and Max O. Wiedorn (CFEL, Univ. Hamburg) for fruitful discussions, and Luigi Adriano (DESY) for technical support. This work was supported by grant of Slovenian Grant Agency (ARRS) J2-7384, Program Group P0-0501-0782 and by Helmholtz Association through project oriented funds.

8 REFERENCES

[1] Chapman, H.N., Fromme, P., Barty, A., White, T.A., Kirian, R.A., Aquila, A., Hunter, M.S., Schulz, J., DePonte, D.P., Weierstall, U., Doak, R.B., Maia, F.R.N.C., Martin, A.V., Schlichting, I., Lomb, L., Coppola, N., Shoeman, R.L., Epp, S.W., Hartmann, R., Rolles, D., Rudenko, A., Foucar, L., Kimmel, N., Weidenspointner, G., Holl, P., Liang, M., Barthelmess, M., Caleman, C., Boutet, S., Bogan, M.J., Krzywinski, J., Bostedt, C., Bajt, S., Gumprecht, L., Rudek, B., Erk, B., Schmidt, C., Hömke, A., Reich, C., Pietschner, D., Strüder, L., Hauser, G., Gorke, H., Ullrich, J., Herrmann, S., Schaller, G., Schopper, F., Soltau, H., Kühnel, K., Messerschmidt, M., Bozek, J.D., Hau-Riege, S.P., Frank, M., Hampton, C.Y., Sierra, R.G., Starodub, D., Williams, G.J., Hajdu, J., Timneanu, N., Seibert, M.M., Andreasson, J., Rocker, A., Jönsson, O., Svenda, M., Stern, S., Nass, K., Andritschke, R., Schröter, C., Krasniqi, F., Bott, M., Schmidt, K.E., Wang, X., Grotjohann, I., Holton, J.M., Barends, T.R.M., Neutze, R., Marchesini, S., Fromme, R., Schorb, S., Rupp, D., Adolph, M., Gorkhover, T., Andersson, I., Hirsemann, H., Potdevin, G., Graafsma, H., B. and Spence, J.C.H. *Femtosecond X-ray protein nanocrystallography.* Nature 470, 73–77, doi: 10.1038/nature09750 (2011).

[2] Beyerlein, K.R., Adriano, L., Heymann, M., Kirian, R., Knoška, J., Wilde, F., Chapman, H.N., and Bajt, S. *Ceramic micro-injection molded nozzles for serial femtosecond crystallography sample delivery.* Review of Scientific Instruments, 86(12), (2015) p.125104. Available at: http://dx.doi.org/10.1063/1.4936843

[3] Nelson, G., Kirian, R.A., Weierstall, U., Zatsepin, N.A., Faragó, T., Baumbach, T., Wilde, F., Niesler, F.B.P., Zimmer, B., Ishigami, I., Hikita, M., Bajt, S., Yeh, S., Rousseau, D.L., Chapman, H.N., Spence, J.C.H., and Heymann, M. *Three-dimensional-printed gas dynamic virtual nozzles for x-ray laser sample delivery*. Opt. Express 24, 11515-11530 (2016)

[4] DePonte, D.P., Weierstall, U., Schmidt, K., Warner, J., Starodub, D., Spence, J.C.H., and Doak, R.B. *Gas dynamic virtual nozzle for generation of microscopic droplet streams*. J. Phys. D 41, 195505 (2008).

[5] Ganán-Calvo, A. M., González-Prieto, R., Riesco-Chueca, P., Herrada, M. A. and Flores-Mosquera, M. *Focusing capillary jets close to the continuum limit.* Nature Physics 3, 737–742, doi: 10.1038/nphys710 (2007).

[6] Oberthuer, D., Knoška J., Wiedorn, M.O., Beyerlein, K.R., Bushnell, D.A., Kovaleva, E.G., Heymann, M., Gumprecht, L., Kirian, R.A., Barty, A., Mariani, V., Tolstikova, A., Adriano, L., Awel, S., Barthelmess, M., Dörner, K., Xavier, P.L., Yefanov, O., James, D.R., Nelson, G., Wang, D., Calvey, G., Chen, Y., Schmidt, A., Szczepek, M., Frielingsdorf, S., Lenz, O., Snell, E., Robinson, P.J., Šarler, B., Belšak, G., Maček, M., Wilde, F., Aquila, A., Boutet, S., Liang, M., Hunter, M.S., Scheerer, P., Lipscomb, J.D., Weierstall, U., Kornberg, R.D., Spence, J.C.H., Pollack, L., Chapman, H.N. and Bajt, S. *Double-flow focused liquid injector for efficient serial femtosecond crystallography.* Sci. Rep. 7, 44628; doi: 10.1038/srep44628 (2017)

[7] Weller, H.G., *A new approach to VOF-based interface capturing methods for incompressible and compressible flow.* Tech.Rep., OpenCFD, 2008.

[8] FreeCAD website: https://www.freecadweb.org/

[9] OpenFoam © 2004-2017 OpenCFD Ltd (ESI Group) website: http://www.openfoam.com/

[10] Ahrens, J., Geveci, B., Law, C. *ParaView: An End-User Tool for Large Data Visualization.* Visualization Handbook, Elsevier, 2005, ISBN-13: 978-0123875822